

RESEARCH

Open Access



Evaluation of microwave square ring metamaterial-based resonator for glucose detection

Muhammad Hakimi Mustafa Kamal¹, Suhail Asghar Qureshi¹, Zuhairiah Zainal Abidin^{1*} , Huda A. Majid¹ and Chan Hwang See²

*Correspondence:
zuhairia@uthm.edu.my

¹ Advanced Telecommunication Research Center (ATRC), Faculty of Electrical and Electronic Engineering, Universiti Tun Hussein Onn Malaysia, Parit Raja, Johor, Malaysia

² Edinburgh Napier University, Edinburgh, UK

Abstract

This study presents a biosensor working at a frequency of 3.5 GHz, which is designed as a square ring metamaterial resonator. This study aimed to evaluate the impact of blood amount on the metamaterial-based resonator sensor's sensitivity. The structure was constructed using Rogers-RT5880 material, with an overall area of 85.71 mm × 85.71 mm². The simulation of the design involved modelling the blood samples using Debye 1st-order equations. The empirical results observed a noticeable shift towards a lower frequency range in the response and changes in the magnitude, corresponding to an increase in the blood sample's glucose concentration and thickness. Following this, the experiment was designed to corroborate the simulated results. The sensor achieved the highest sensitivity of 0.23 dB per 100 mg/dl change in glucose level when the thickness of blood was 0.1 mm. It was concluded from the results that the increase in the volume of blood increases the sensor's sensitivity. However, a trade-off mark is necessary in which an optimum sensitivity is achieved with blood volume as minimum as possible so that a noninvasive biosensor can be designed.

Keywords: Metamaterial, Resonator, Glucose, Sensing

Introduction

Diabetes mellitus (DM) is one of the leading causes of global casualties. It is estimated that DM reduces the life of the average person by roughly 4–8 years [1]. Effective management of diabetes management critically requires frequent glucose measurements. According to healthcare guidelines, glucose needs to be monitored four times a day, which may increase up to ten times in case of poor diabetic conditions [2]. Several methods have been proposed to date for glucose monitoring that employ optical, electrochemical, and microwave technologies. Optical technology is used in terms of polarized optical rotation, near-infrared reflectance spectroscopy (NIRS), optical coherence tomography (OCT), fluorescence, Raman spectroscopy, etc. [3–7]. In recent times, radio frequency (RF)/microwave technology has been presented extensively for minimal bio-sensing, which relies on the principle of dielectric characterization. This means these systems detect permittivity changes due

to the changes in glucose concentration of target cells or tissues [8]. In addition, this technology offers harmless penetration of electromagnetic (EM) waves in contrast to X-rays and other ionizing radiations. Microwave devices are useful in the near-field monitoring of biomaterials [9]. The interest in the characterization of EM properties has increased exponentially in the last decade beyond glucose sensing in a variety of industrial, agricultural, chemical, and medical applications. Microwave detection techniques have proved to be portable, cost-effective, label-free, and able to integrate with advanced systems such as the Internet of Things (IoT) [10–12]. Among the characterization methods, resonant-based biosensors offer quick and effective dielectric permittivity measurements with good accuracy and precision in the sensing measurements [13]. The principle of these structures relies on the traces of resonance and changes in its quality factor, resonant frequency, and amplitude with respect to the dielectric variations in biological tissues. Recently studied biosensors based on transmission and/or reflection coefficient mechanisms include mediator-free resonators [14], substrate-integrated waveguide cavity resonators [15], closed-loop enclosed split ring resonators [16], microstrip antenna-driven ring resonators [17], plasmonic metamaterial-based sensor [18], and microstrip line [19]. In glucose sensing, a major pitfall has been sensitivity, the effect of environmental interferences, and cross-sensitivity. Nevertheless, major contributions have been made by various authors in these aspects. For example, a T-shaped patterned signal line-based sensor was presented in [20] to detect glucose concentration in blood. The transmission line pattern was created to enhance the sensitivity via greater interaction of fields with the subject under test. A model of in vitro glucose measurement was presented in [21] using a cavity sensor, which could detect D-glucose in pig blood from a concentration of 150 to 550 mg/dl. However, it was realized that glucose concentrations are highly affected by temperature variations. In this aspect, the realization of compact, high-sensitive, low-cost, miniaturized glucose sensing has been studied by various authors who integrated artificially engineered materials having unique properties in microwave circuits [22–24]. The sensitivity of the microwave sensors has been reported to increase with the incorporation of the metamaterial due to the integrated system's stronger electric field and magnetic field interaction with the sample under test (SUT). For the detection and rapid monitoring of blood glucose concentration with high sensitivity, a new metamaterial-based sensor is proposed in this paper. Measurement of the concentration of glucose in the blood with the help of a metamaterial sensor can be considered an efficient method that potentially fulfils its criteria of being highly sensitive [3]. This technique is based on the blood's dielectric response to changing glucose concentration [25]. A major drawback experienced in glucose sensing is the amount of blood required to estimate the corresponding glucose level. Therefore, in this study, an effort has been made to analyze to what extent does volume of blood affects the sensitivity of metamaterial-based sensor in detecting blood glucose. For that purpose, a metamaterial-based sensor operating at 3.5-GHz frequency has been designed and tested on blood. Later, sensitivity analysis is conducted to determine the sensor's sensitivity based on the glucose level of the blood as well as its volume.

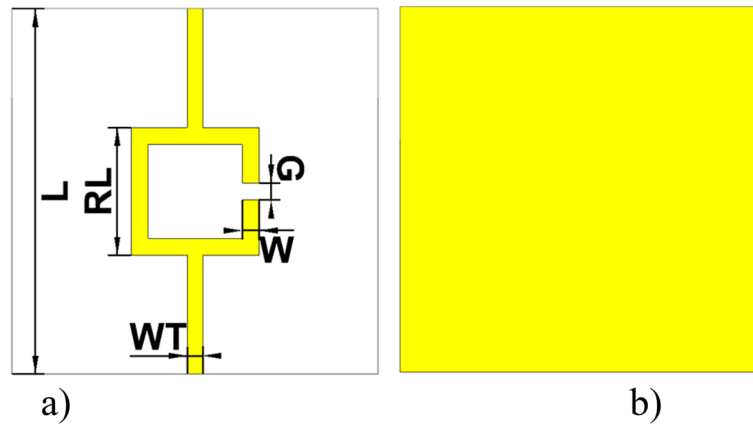


Fig. 1 Proposed microstrip square ring resonator. **a** Top view and **b** bottom view for resonance at 3.5 GHz

Table 1 The proposed dimension in mm

Parameter	Dimension in mm
L	85.71
RL	30
WT	3.65
G	4
h	1.47
t	0.035

Methods

3D design and simulation setup

Figure 1 depicts the proposed square ring resonator design with two microstrip lines operating at 3.5 GHz. The sensor structure is constructed on Rogers-RT5880 with a dielectric constant (ϵ) of 2.2 and tangent loss (δ) of 0.0009. The sensor has been designed on a conventional metal-dielectric-metal configuration with the top layer of copper being designed as a resonator and the bottom layer acting as a conductor. The thickness of the substrate (h) is 1.47 mm, whereas copper metal has a thickness (t) of 0.035 mm. A feed transmission line is connected to a resonating structure whose width (WT) was calculated using Eq. 1. The optimal dimension of the proposed design is depicted in Table 1. The proposed design was simulated and analyzed using CST Studio simulation software (Fig. 2). A pair of ports were designed at ends of feed transmission lines, and simulation was carried out in time domain from 1 to 5 GHz frequency.

$$WT = \frac{7.48 \times h}{e^{\left(\frac{Z_0 \sqrt{\epsilon_r + 1.41}}{87}\right)}} - 1.25 \times t \quad (1)$$

Blood and other aqueous fluids exhibit dispersion characteristics with frequency-dependent electromagnetic properties. This section will examine the relationship between the frequency and complex permittivity of the blood. The mathematical characterization of the phenomenon was achieved through the utilization of the Debye models. The complex

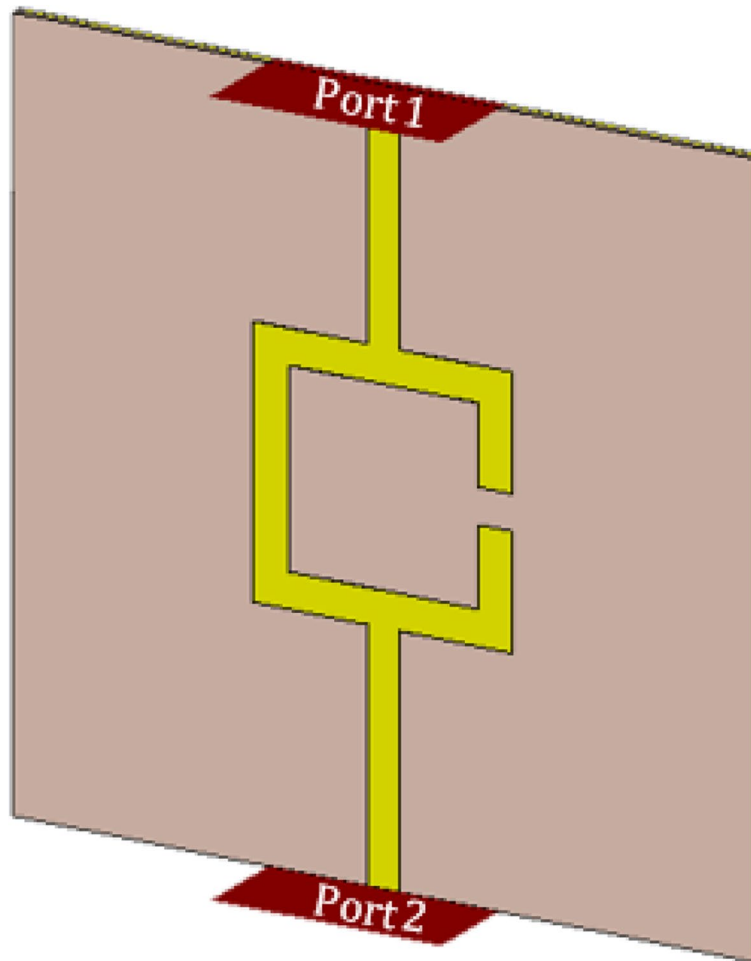


Fig. 2 Simulation setup with two ports

permittivity of any material can be characterized using Debye parameters, as demonstrated in Eq. 2 [26].

$$\varepsilon(\omega) = \varepsilon_{\infty} + \frac{\varepsilon_s - \varepsilon_{\infty}}{1 + j\omega\tau} \quad (2)$$

where τ is the relaxation time in picoseconds, whereas static permittivity and high-frequency permittivity are expressed by ε_s and ε_{∞} , respectively. In this work, single-order Debye model parameters were used to model the blood's dielectric characteristics in simulations as a function of glucose concentration. Debye parameters of samples as a function of glucose concentrations were calculated using Eqs. (3–4) [27].

$$\varepsilon_{\infty}(G) = 5.38 + G \times 30 \times 10^{-3} \quad (3)$$

$$\varepsilon_s(G) = 80.68 + G \times 0.207 \times 10^{-3} \quad (4)$$

$$\tau(G) = 9.68 + G \times 0.23 \times 10^{-3} \quad (5)$$

where G is the glucose concentration in milligrams per deciliter (mg/dl). The blood's dispersive characteristics as a function of glucose content are modelled for glucose concentrations of 80, 100, 120, and 140 mg/dl. The results are then fitted to the single-pole Debye empirical model in CST Studio Suite software for sensor simulations to evaluate their performance.

Validation of metamaterial-based resonator structure

Metamaterial is a term used for artificially developed materials exhibiting unnatural properties. These materials offer negative permittivity and permeability simultaneously. A robust retrieval method [28] was used to extract the constitutive parameters (permittivity and permeability) of the metamaterial structure. As illustrated in Fig. 3, the designed structure for the proposed resonator produces a negative refractive index when its permeability and permittivity are negative at its resonance frequency (3.5 GHz). As a result, the proposed design displays the metamaterial's double-negative features (DNG).

Fabrication and measurement setup

To validate the simulated result, the proposed structure was fabricated, and the structure's fabrication is depicted in Fig. 4. As the figure shows, the resonator is connected to two subminiature version-A (SMA) connectors via a feed transmission line. Later, the SMA connectors were connected to the Rohde and Schwarz ZNB20 Vector Network Analyzer (VNA) to carry out the measurements. The reflection coefficient response, S_{11} , of the resonator was observed through the VNA, as depicted previously in Fig. 5. Samples were obtained using the finger prick technique. Four individuals served as volunteers, resulting in a total of four blood samples. The demographic information of the volunteer, including age, height, weight, and blood glucose levels, was collected. The primary point of reference for assessing glucose levels was glucometer. Next, blood glucose levels were assessed through the designed metamaterial resonator sensor. The

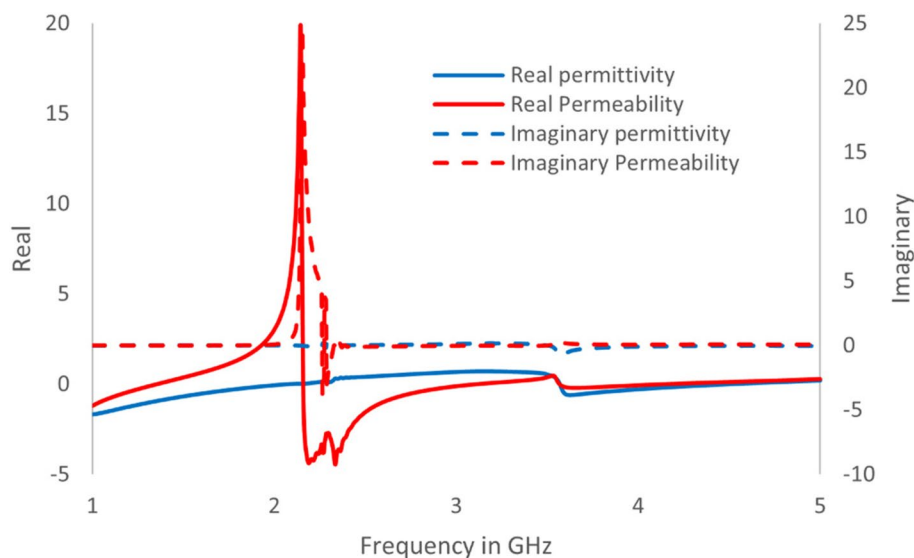


Fig. 3 The permittivity and permeability of the proposed resonator

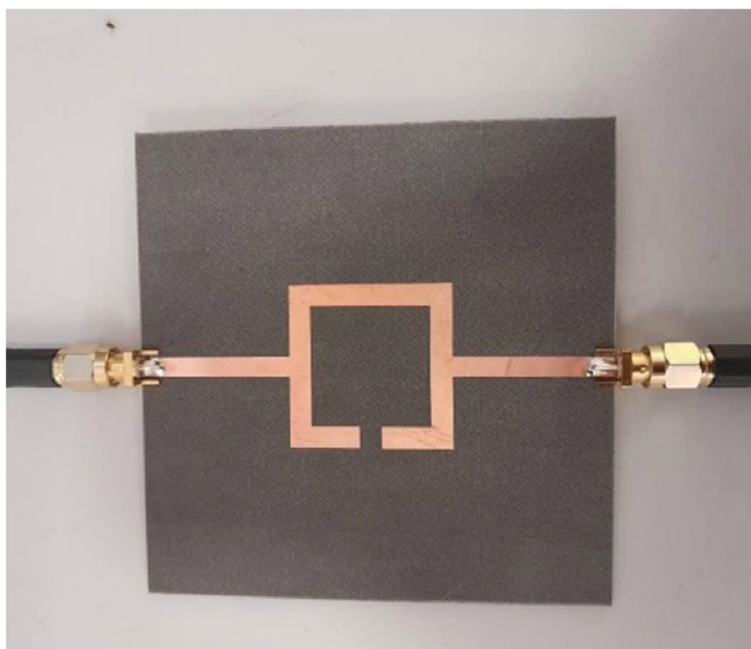


Fig. 4 Proposed resonator with probe connection

resonator's gap was filled with the blood samples, and responses of S-parameters were analyzed.

Results and discussion

The electric field was analyzed to understand the designed operating principle. As depicted in Fig. 6, the electric field distribution was observed through Port 1 at the resonance frequency of 3.5 GHz without the absence of a sample. The graphs illustrate that the electric field intensity is mainly concentrated on the transmitted side of every port. Moreover, the gap created in the square ring resonator is a primary area of interest in the electric field distribution. The field strength level observed near the gap provides evidence supporting this hypothesis. Consequently, the resonator's gap can identify the changes in dielectric characteristics with the highest sensitivity.

Simulated and measured results

The metamaterial-based resonator is essentially a capacitive resonance unit with high efficiency in the microwave frequency band. With electromagnetic excitation, the induced current will be generated on the metal, which causes the inductive effect, while a gap/cut in the shape of a resonator results in a capacitive coupling effect. Therefore, the resonant frequency of the unit cell modelled can be expressed in terms of equivalent capacitance (C_c) and inductance (L_0) as given in Eq. (6).

$$f = \frac{1}{\sqrt{L_0 C_c}} \quad (6)$$

The reflection coefficient (S_{11}) of the design is shown in Fig. 7, where a comparison is made between simulated and measured results. The structure resonates at approximately

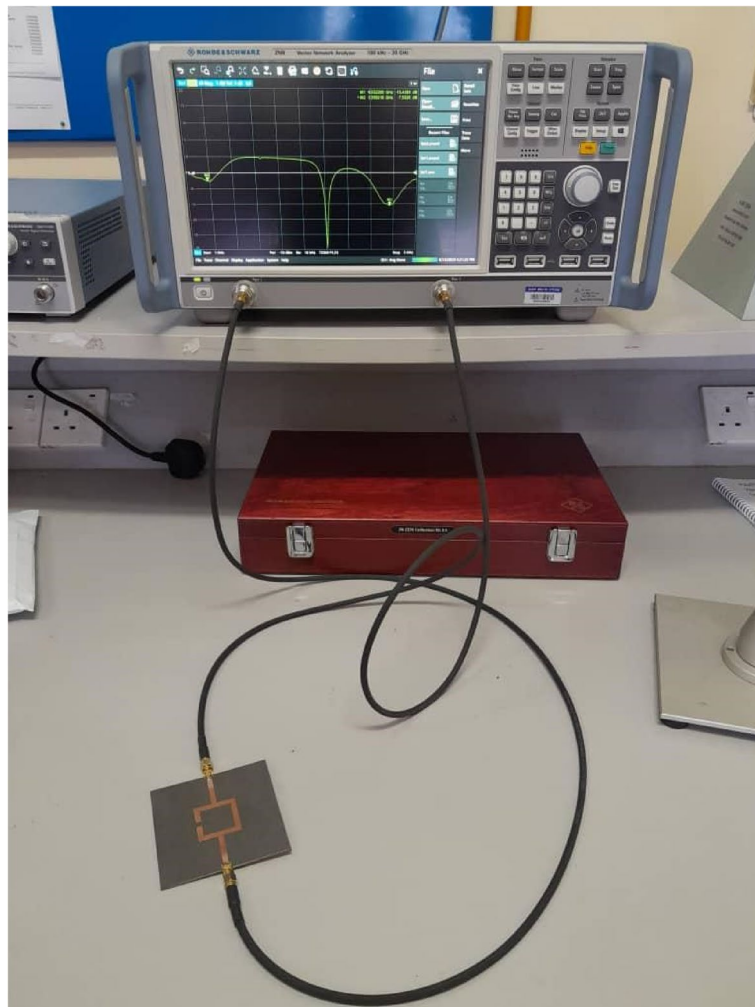


Fig. 5 Measurement setup

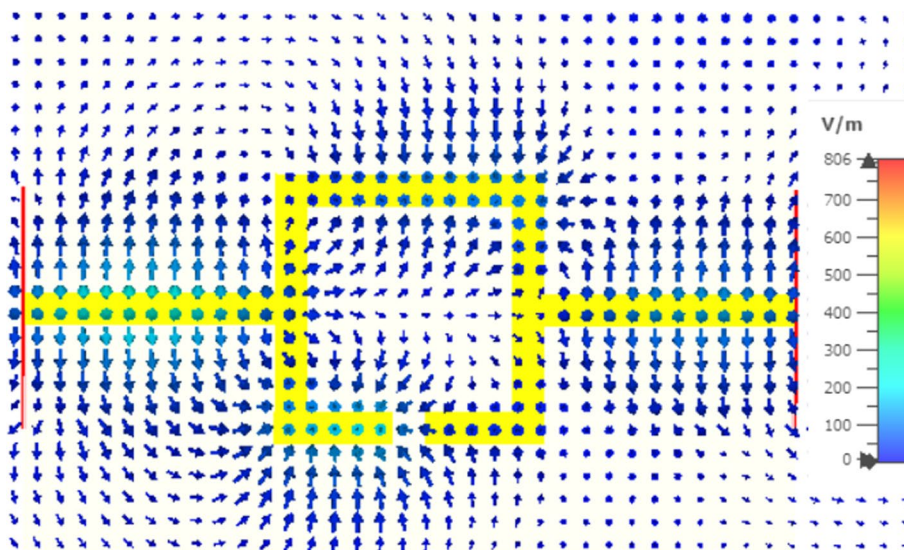


Fig. 6 Electric field distribution on Port 1

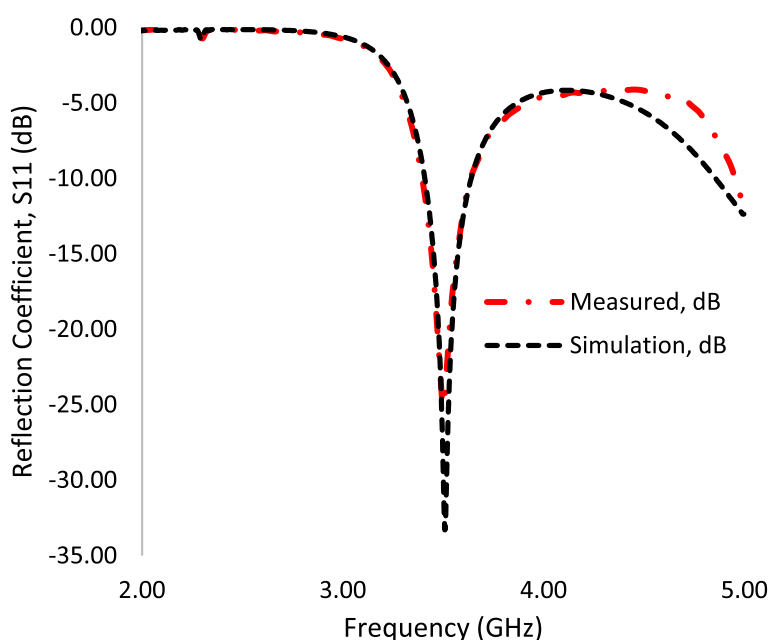


Fig. 7 The simulated and measured reflection coefficient (S_{11}) of the proposed structure without sample

3.508 GHz. The results show a good agreement between the simulated data and the measurement results. A small discrepancy is observed between simulated and measured results, which is mainly contributed by the environmental factors and soldering of the SMA connectors to the feed transmission lines.

The performance of the fabricated resonator was evaluated through the testing of the blood of four volunteers with different blood glucose levels. The glucose level of blood was obtained using the finger prick technique and tested with an Accu-Chek glucometer, as shown in Fig. 8. Table 2 shows that the volunteers in this study are male whose glucose level, age, height, and weight were recorded. The glucose levels of the volunteers are assessed utilizing a glucose meter and acquired in units of millimoles per liter (mmol/L). The glucose unit was converted to milligrams per deciliter (mg/dL) to compare unit values within measurement and simulation. Following the acquisition of results, the blood sample underwent an examination on the designed sensor to observe the changes in the reflection coefficient (S_{11}). Coincidentally, the glucose level readings obtained from the



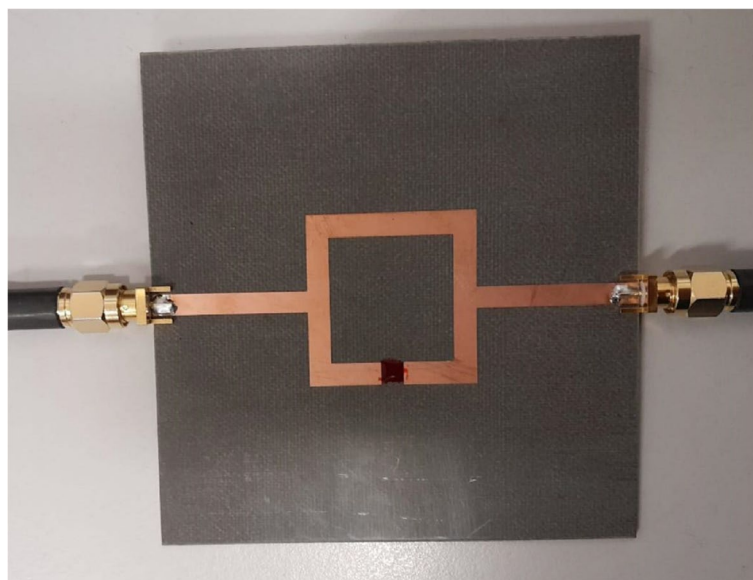
Fig. 8 The glucose level of the samples

Table 2 The data of the volunteers

Sample	Gender	Age	Height (cm)	Weight (kg)	Glucose level (mmol/L)	Glucose level (mg/dL)
1	Male	28	165	65	4.6	79.2
2	Male	25	168	60	5.7	102.6
3	Male	25	172	70	6.5	117
4	Male	42	168	60	7.8	140.4

glucose meter device returned approximately equal to the glucose concentration levels assumed during simulations. Following the acquisition of glucometer readings, the sensor's resonance was analyzed on the application of those blood samples.

The blood sample was placed in the gap of the square resonator, as shown in Fig. 9. The changes can be observed in terms of resonance frequency and its magnitude with respect to the changes in glucose level, as depicted in Fig. 10. In the context of this measurement situation, it is not feasible to quantify blood thickness directly. However, it is possible to deduce that the small number of blood droplets on the sensor impacts the resonance frequency and magnitude. For this reason, the resonance recorded for sample 1 with a glucose level of 79.2 and sample 4 with a glucose level of 140.2 has almost the same resonance frequency at 3.46 GHz which could happen due to the higher volume of sample 1. Meanwhile, sample 2 has the highest resonance frequency which is 3.48 GHz, and sample 3 has the lowest resonance frequency which is 3.42 GHz. However, it can be realized from the results that with the shifting of resonance towards lower frequencies, the magnitude of resonances tends to be increasing consistently. It shows that the shift in resonance could be obtained linearly with respect to glucose levels provided that the volume of the blood sample is as accurate as possible. This phenomenon of decreasing resonance with increased glucose concentration has

**Fig. 9** Resonator testing with a blood sample

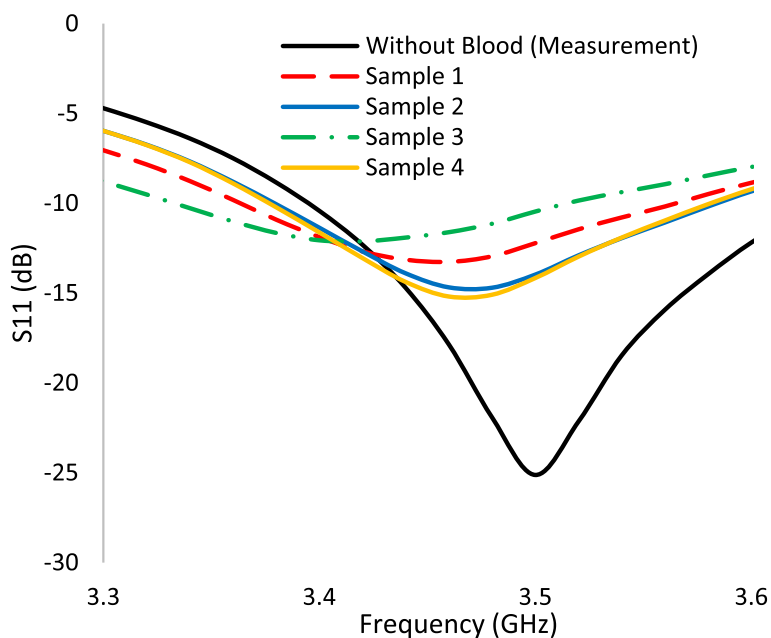


Fig. 10 Measured reflection coefficient responses of different blood samples

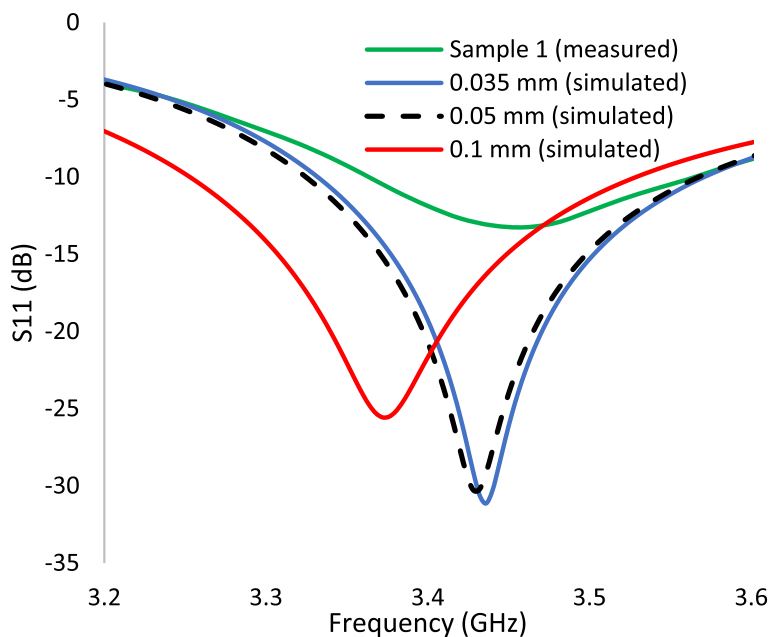


Fig. 11 Comparison between measured and simulated reflection coefficient responses of different blood thickness at 80 mg/dL

also been reported in previous studies [16, 29, 30]. Additional analysis was conducted by varying the thickness of the sample to 0.035 mm, 0.05 mm, and 0.1 mm in the simulations. Figures 11, 12, 13, and 14 represent the comparison of the simulated and measured results. The volume of the sample at a constant glucose level shifts the resonance towards a lower frequency. The sample's thickness of 0.1 mm has the lowest resonance,

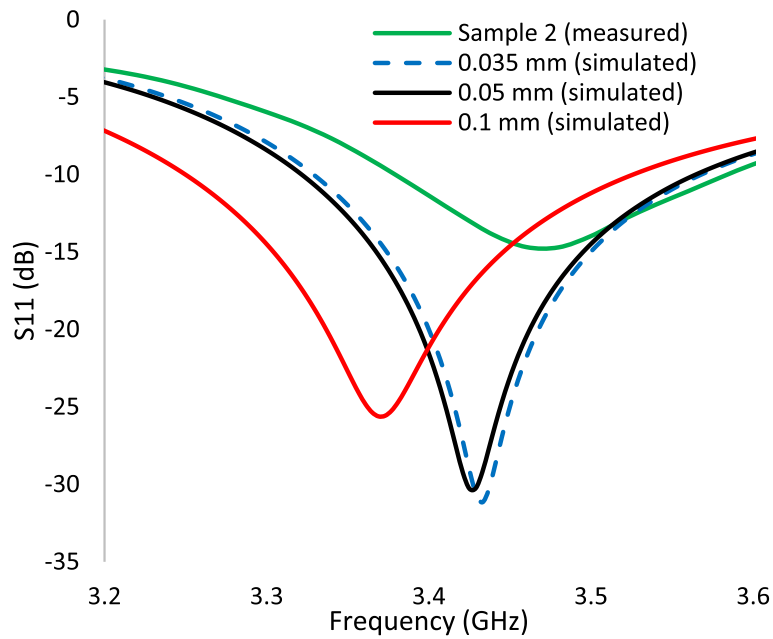


Fig. 12 Comparison between measured and simulated reflection coefficient responses of different blood thickness at 100 mg/dL

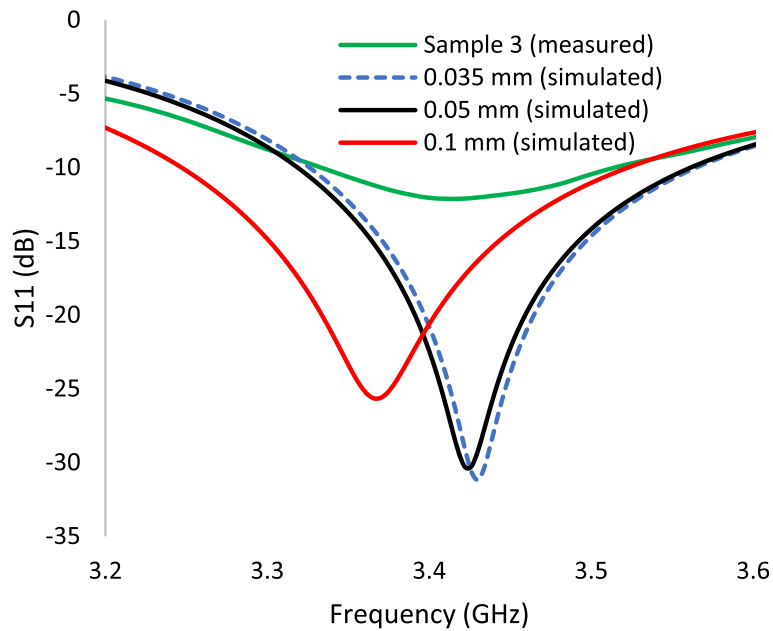


Fig. 13 Comparison between measured and simulated reflection coefficient responses of different blood thickness at 120 mg/dL

and 0.035 mm thickness has the highest resonance at all glucose levels recorded in this study. Even though the sample's thickness cannot be quantified, the observed results appear to follow the simulation patterns, in which the resonance frequency shifts to lower frequencies as the blood glucose level increases.

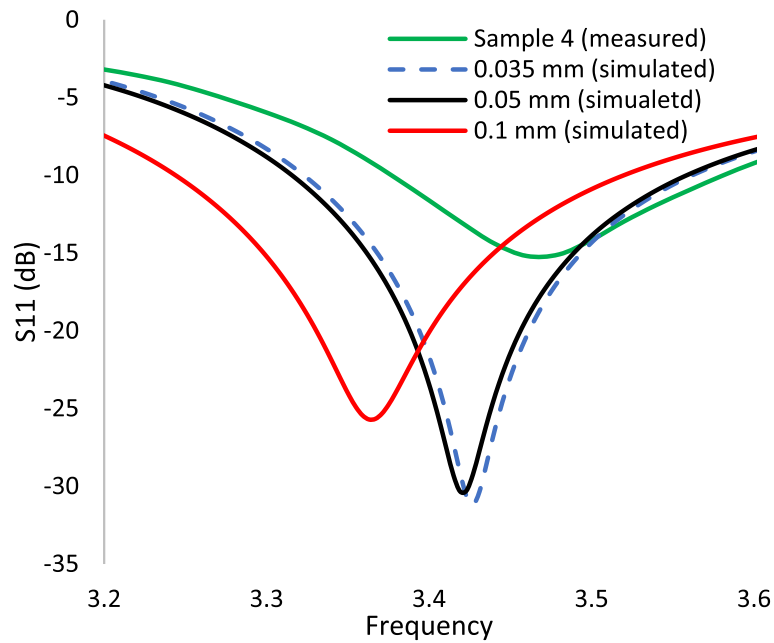


Fig. 14 Comparison between measured and simulated reflection coefficient responses of different blood thickness at 140 mg/dL

Sensitivity analysis

In this section, the sensitivity of the sensor is determined depending on the glucose level as well as the volume of blood. The sensitivity can be calculated by using Eq. 7:

$$S = \lim_{\Delta(U_h - U_l) \rightarrow 0} \frac{\Delta f_{sh} - \Delta f_{sl}}{\Delta U_h - \Delta U_l} \tag{7}$$

where Δf_{sh} represents the highest shift in resonant frequency and Δf_{sl} represents the lowest shift in resonant frequency, ΔU_h represents the highest change in unit (either glucose or volume), and ΔU_l represents the lowest change in units. The highest and lowest thickness of glucose values considered in this study are 1.0 mm and 0.035 mm, respectively, and their corresponding resonances are 3.372 GHz and 3.436 GHz. Considering the resonance to be at 3.508 GHz, the sensitivity in terms of the thickness of blood is determined as 0.066 per unit change in mm. On the other hand, even though there is no clear shift in resonance when the glucose level is changed, a distinct change in the magnitude of the reflection coefficient can be seen. Therefore, the designed sensor’s sensitivity based on glucose levels is calculated using S_{11} magnitude at each resonance frequency observed for different samples. In that case, Δf_{sh} can be replaced by dB_{sh} and dB_{sl} which represents the magnitude of S_{11} at resonances of the highest glucose level (140 mg/dl) and lowest glucose level (80 mg/dl). If a blood sample of 0.1 mm thickness is to be assumed, the sensor’s sensitivity is determined as 0.23 dB per 100 mg/dl change in glucose level. In case blood samples of 0.5 mm thickness are assumed, the sensitivity is calculated as 0.12 dB per 100 mg/dl change in glucose level, and sensitivity in case of 0.035 mm thickness of blood is 0.095 dB per 100 mg/dl change in glucose level. This shows that the increase in the volume of blood increases the sensitivity of the sensor. Moreover, for further examination of these results, a linear regression model

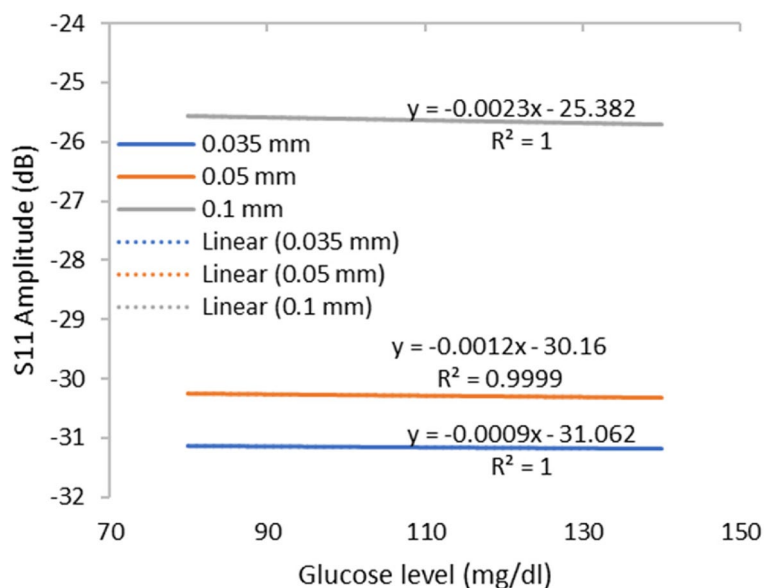


Fig. 15 Fitting curve for the different thickness of blood sample

Table 3 Comparison of the designed sensor with state-of-the-art sensors

Reference	Operating frequency (GHz)	Glucose range (mg/dl)	Sensing parameter	Sensitivity (dB/100 mg/dl)
[27]	3.1	60–300	S_{21}	1.67
[33]	2.4–2.9	0–400	S_{21}	0.0075
[31]	2	0–250	S_{21}	0.71
[32]	25.56	50–120	S_{21}	2.7
[34]	6.5	0–40,000	S_{21}	0.19
[35]	2.35	70–130	S_{11}	0.2
This paper	3.5	80–140	S_{11}	0.23

is presented, which can be useful for the data that are not used in this study based on the fitting curve. Figure 15 shows the fitting curve of the change in S_{11} magnitude with respect to the changes in glucose levels at various thicknesses of the blood sample. The R^2 value for the regression model applied is 1 which shows perfect linearity in the changes in magnitude of S_{11} with respect to the changes in glucose levels. In Table 3, the performance of the designed sensor is compared with the state-of-the-art sensors. It can be seen that the sensitivity of the designed sensor is better than most of the sensors. However, it was also apparent that the increase in volume increases the sensitivity of glucose detection, which is why the sensitivity reported in [31] and [27] is better. On the other hand, an increase in frequency also leads to sensitivity enhancement. Therefore, the sensitivity reported in [32] is significantly higher than other reported sensors.

Conclusions

The numerical methodology employed in this study involves the utilization of a proposed resonator that relies on a metamaterial (MTM) design for blood detection. By monitoring the variation in S_{11} , the proposed configuration has the potential to differentiate between different blood glucose concentrations. The proposed structure of the resonator was designed and subjected to experimental evaluation. An effort was made to analyze the effect of the blood's volume on the sensitivity of the sensor, which showed the direct relationship of the sensor's sensitivity with the blood's volume. However, a trade-off mark should be decided when it is a matter of health, and blood used for testing is as minimal as possible so that noninvasive glucose monitoring could be possible. The proposed design indicates the predicted model is reliable. In future, the design can be improved by resizing and integrating it with the communication module for commercialization purposes.

Abbreviations

DM	Diabetes mellitus
NIRS	Near-infrared reflectance spectroscopy
OCT	Optical coherence tomography
RF	Radio frequency
EM	Electromagnetic
IoT	Internet of Things
SUT	Sample under test
mg/dl	Milligrams per deciliter
SMA	Subminiature version A
VNA	Vector Network Analyzer
mmol/L	Millimoles per liter
MTM	Metamaterial

Acknowledgements

The authors would like to extend their sincere appreciation to Universiti Tun Hussein Onn Malaysia (UTHM) for their support and encouragement throughout the research process.

Authors' contributions

MH carried out simulation and experimental work and writing of the manuscript. ZZ thoroughly supervised the project. SA assisted in revising the manuscript. HA helped in carrying out experimental work. CH helped in proofreading the manuscript. All authors read and approved the final manuscript.

Funding

This research was supported by Universiti Tun Hussein Onn Malaysia (UTHM) through TIER 1 (Vot Q161).

Availability of data and materials

The corresponding author can be contacted for any related data.

Declarations

Ethics approval and consent to participate

The participants had given their consent. In addition, this work has been approved by the Research Ethics Committee (REC), UTHM.

Competing interests

The authors declare that they have no competing interests.

Received: 7 September 2023 Accepted: 11 January 2024

Published online: 05 March 2024

References

1. Wander GS, Bansal M, Kasliwal RR (2020) Prediction and early detection of cardiovascular disease in South Asians with diabetes mellitus. *Diabetes Metab Syndr Clin Res Rev* 14(4):385–393. <https://doi.org/10.1016/j.dsx.2020.04.017>
2. "Standards of Medical Care in Diabetes--2010," *Diabetes Care*, vol. 33, no. Supplement_1, pp. S11–S61, Jan. 2010, doi: <https://doi.org/10.2337/dc10-S011>

3. Siddiqui SA, Zhang Y, Lloret J, Song H, Obradovic Z (2018) Pain-Free blood glucose monitoring using wearable sensors: recent advancements and future prospects. *IEEE Rev Biomed Eng* 11:21–35. <https://doi.org/10.1109/RBME.2018.2822301>
4. Villena Gonzales W, Mobashsher A, Abbosh A (2019) The progress of glucose monitoring—a review of invasive to minimally and non-invasive techniques, devices and sensors. *Sensors* 19(4):800. <https://doi.org/10.3390/s19040800>
5. Amir O, Weinstein D, Zilberman S, Less M, Perl-Treves D, Primack H, Weinstein A, Gabis E, Fikhte B, Karasik A (2007) Continuous noninvasive glucose monitoring technology based on 'occlusion spectroscopy.' *J Diabetes Sci Technol* 1(4):463–469. <https://doi.org/10.1177/193229680700100403>
6. Shokrehodaie M, Quinones S (2020) Review of non-invasive glucose sensing techniques: optical, electrical and breath acetone. *Sensors* 20(5):1251. <https://doi.org/10.3390/s20051251>
7. Haxha S, Jhoja J (2016) Optical based noninvasive glucose monitoring sensor prototype. *IEEE Photonics J* 8(6):1–11. <https://doi.org/10.1109/JPHOT.2016.2616491>
8. Hassan RS, Lee J, Kim S (2020) A minimally invasive implantable sensor for continuous wireless glucose monitoring based on a passive resonator. *IEEE Antennas Wirel Propag Lett* 19(1):124–128. <https://doi.org/10.1109/LAWP.2019.2955176>
9. Choi H, Naylon J, Luzio S, Beutler J, Birchall J, Martin C, Porch A (2015) Design and in vitro interference test of microwave noninvasive blood glucose monitoring sensor. *IEEE Trans Microw Theory Tech* 63(10):3016–3025. <https://doi.org/10.1109/TMTT.2015.2472019>
10. Saghlatoon H, Mirzavand R, Honari MM, Mousavi P (2018) Sensor antenna transmitter system for material detection in wireless-sensor-node applications. *IEEE Sens J*. <https://doi.org/10.1109/JSEN.2018.2868006>
11. Sharafadinzadeh N, Abdolrazzaghi M, Daneshmand M (2020) Investigation on planar microwave sensors with enhanced sensitivity from microfluidic integration. *Sensors Actuators A Phys* 301:111752. <https://doi.org/10.1016/j.sna.2019.111752>
12. Chudpooti N, Duangrit N, Sangpet P, Akkaraekthalin P, Imberg BU, Robertson ID, Somjit N (2020) In-situ self-aligned NaCl-solution fluidic-integrated microwave sensors for industrial and biomedical applications. *IEEE Access* 8:188897–188907. <https://doi.org/10.1109/ACCESS.2020.3031864>
13. Ansari MAH, Jha AK, Akhtar MJ (2015) Design and application of the CSRR-based planar sensor for noninvasive measurement of complex permittivity. *IEEE Sens J* 15(12):7181–7189. <https://doi.org/10.1109/JSEN.2015.2469683>
14. Kumar A, Wang C, Meng FY, Zhou ZL, Zhao M, Yan GF, Kim ES, Kim NY (2020) High-sensitivity, quantified, linear and mediator-free resonator-based microwave biosensor for glucose detection. *Sensors (Switzerland)* 20(14):1–17. <https://doi.org/10.3390/s20144024>
15. Salim A, Kim SH, Park JY, Lim S (2018) Microfluidic biosensor based on microwave substrate-integrated waveguide cavity resonator. *J Sensors* 2018:1–13. <https://doi.org/10.1155/2018/1324145>
16. Kandwal A, Igbe T, Li J, Liu Y, Li S, Liu LWY, Nie Z (2020) Highly sensitive closed loop enclosed split ring biosensor with high field confinement for aqueous and blood-glucose measurements. *Sci Rep* 10(1):4081. <https://doi.org/10.1038/s41598-020-60806-9>
17. Camli B, Kusakci E, Lafci B, Salman S, Torun H, Yalcinkaya AD (2017) Cost-effective, microstrip antenna driven ring resonator microwave biosensor for biospecific detection of glucose. *IEEE J Sel Top Quantum Electron* 23(2):404–409. <https://doi.org/10.1109/JSTQE.2017.2659226>
18. Pandit N, Jaiswal RK, Pathak NP (2020) Plasmonic metamaterial-based label-free microfluidic microwave sensor for aqueous biological applications. *IEEE Sens J* 20(18):10582–10590. <https://doi.org/10.1109/JSEN.2020.2994061>
19. Li L, Uttamchandani D (2009) A microwave dielectric biosensor based on suspended distributed MEMS transmission lines. *IEEE Sens J* 9(12):1825–1830. <https://doi.org/10.1109/JSEN.2009.2031388>
20. Omkar YU, Huang SY (2018) T-shaped patterned microstrip line for noninvasive continuous glucose sensing. *IEEE Microw Wirel Components Lett* 28(10):942–944. <https://doi.org/10.1109/LMWC.2018.2861565>
21. Kim S, Melikyan H, Kim J, Babajanyan A, Lee JH, Enkhtur L, Friedman B, Lee K (2012) Noninvasive in vitro measurement of pig-blood d-glucose by using a microwave cavity sensor. *Diabetes Res Clin Pract* 96(3):379–384. <https://doi.org/10.1016/j.diabres.2012.01.018>
22. Chen T, Li S, Sun H (2012) Metamaterials application in sensing. *Sensors* 12(3):2742–2765. <https://doi.org/10.3390/s120302742>
23. Su L, Mata-Contreras J, Vélez P, Martín F, Vivek A, Shambavi K, Alex ZC, Omer AE, Shaker G, Safavi-Naeini S, Shubair RM, Hughson R, Shaker G, Vrba J, Vrba D (2019) A review of sensing strategies for microwave sensors based on metamaterial-inspired resonators: dielectric characterization, displacement, and angular velocity measurements for health diagnosis, telecommunication, and space applications. *Int J Antennas Propag* 2017:1–13. <https://doi.org/10.1155/2017/5619728>
24. Singh G, Ni R, Marwaha A (2015) A review of metamaterials and its applications. *Int J Eng Trends Technol* 19(6):305–310. <https://doi.org/10.14445/22315381/IJETT-V19P254>
25. A. E. Omer, G. Shaker, S. Safavi-Naeini, R. M. Shubair, "EM measurements of glucose-aqueous solutions," in 2019 IEEE International Symposium on Antennas and Propagation and USNC-URSI Radio Science Meeting, Jul. 2019;103–104. <https://doi.org/10.1109/APUSNCURSINRSM.2019.8888307>
26. Gabriel S, Lau RW, Gabriel C (1996) Physics in Medicine & Biology. The dielectric properties of biological tissues: III. Parametric models for the dielectric spectrum of tissues. *Phys Med Biol* 41(11):2271–2293. <https://doi.org/10.1088/0031-9155/41/11/003>
27. Omer AE, Shaker G, Safavi-Naeini S, Alquie G, Deshours F, Kokabi H, Shubair RM (2020) Non-invasive real-time monitoring of glucose level using novel microwave biosensor based on triple-pole CSRR. *IEEE Trans Biomed Circuits Syst* 14(6):1407–1420. <https://doi.org/10.1109/TBCAS.2020.3038589>
28. Chen X, Grzegorzczak TM, Wu BI, Pacheco J, Kong JA (2004) Robust method to retrieve the constitutive effective parameters of metamaterials. *Phys Rev E Stat Physics, Plasmas, Fluids, Relat Interdiscip Top* 70(1):7. <https://doi.org/10.1103/PhysRevE.70.016608>
29. Govind G, Akhtar MJ (2019) Metamaterial-inspired microwave microfluidic sensor for glucose monitoring in aqueous solutions. *IEEE Sens J* 19(24):11900–11907. <https://doi.org/10.1109/JSEN.2019.2938853>

30. Islam MT, Hoque A, Almutairi AF, Amin N (2019) Left-handed metamaterial-inspired unit cell for S-band glucose sensing application. *Sensors* 19(1):169. <https://doi.org/10.3390/s19010169>
31. Vrba J, Vrba D (2015) A microwave metamaterial inspired sensor for non-invasive blood glucose monitoring. *Radio-engineering* 24(4):877–884. <https://doi.org/10.13164/re.2015.0877>
32. Qureshi SA, Abidin ZZ, Elamin NIM, Majid HA, Ashyap AYI, Nebhen J, Kamarudin MR, See CH, Abd-Alhameed RA (2022) Glucose level detection using millimetre-wave metamaterial-inspired resonator. *PLoS ONE* 17(6):e0269060. <https://doi.org/10.1371/journal.pone.0269060>
33. Jang C, Park J-K, Lee H-J, Yun G-H, Yook J-G (2020) Non-invasive fluidic glucose detection based on dual microwave complementary split ring resonators with a switching circuit for environmental effect elimination. *IEEE Sens J* 20(15):8520–8527. <https://doi.org/10.1109/JSEN.2020.2984779>
34. J. A. Byford, K. Y. Park, and P. Chahal, "Metamaterial inspired periodic structure used for microfluidic sensing," in 2015 IEEE 65th Electronic Components and Technology Conference (ECTC), 2015;1997–2002. <https://doi.org/10.1109/ECTC.2015.7159876>
35. H. M. Marzouk, A. S. A. El-Hameed, A. Allam, and A. B. Abdel-Rahman, "Design of non-invasive glucose measurement sensor," in 2022 10th International Japan-Africa Conference on Electronics, Communications, and Computations (JAC-ECC), 2022;212–215. <https://doi.org/10.1109/JAC-ECC56395.2022.10043973>

Publisher's Note

Springer Nature remains neutral with regard to jurisdictional claims in published maps and institutional affiliations.